Ultrafast Relaxation Dynamics from the S_2 State of Malachite Green Studied with Femtosecond Upconversion Spectroscopy

Achikanath C. Bhasikuttan,[†,‡,§] Avinash V. Sapre,*[,‡] and Tadashi Okada*[,†]

Department of Chemistry, Graduate School of Engineering Science, Osaka University, Toyonaka, Osaka 560 8531, Japan, and Radiation Chemistry and Chemical Dynamics Division, Bhabha Atomic Research Centre, Trombay, Mumbai 400 085, India

Received: February 26, 2003

We have studied the relaxation dynamics in a triphenyl methane (TPM) dye, malachite green (MG), following S_2-state excitation using fluorescence up-conversion measurements in ethanol and ethylene glycol solutions. Information on the mechanisms and dynamics of radiationless transitions from higher excited states in TPM dyes is interesting from the torsional dynamic aspects of the phenyl rings and for the applications of TPM dyes involving knowledge of the excited-state relaxation channels. Kinetic measurements at different wavelengths suggested a cascade population relaxation along the S_2 state with a time constant of ∼130 fs that is almost independent of solvent viscosity in the two solvents used, contrary to the relaxation dynamics of the S_1 state. Wavelength-dependent time-resolved anisotropy measurements along the S_2 and S_1 emission bands displayed successive reductions in the anisotropy values, indicating a continuous evolution to the S_1 surface. A detailed analysis led us to propose a relaxation pathway along a surface contact of S_2 and S_1 potential surfaces, generally known as conical intersection, which leads to characteristics of mixed vibrational levels of S_2 and S_1. We propose that the conical intersection is promoted by a torsional coordinate of the unsubstituted phenyl ring of the dye, where the S_2 transition energy is localized. The proposal of a conical intersection between the S_2 and S_1 potential surfaces provides first-hand information on such a model in TPM dyes, which is substantially supported by time-resolved anisotropy measurements.

1. Introduction

Triphenyl methane (TPM) dyes have received considerable attention in physical chemistry from both fundamental and applied research.[1] These dyes have been long studied for their molecular structure, electronic states, and relaxation dynamics.[1−10] The photoprocesses in TPM dyes are intrinsically interesting but complicated and have been extensively investigated using various time-resolved techniques.[1−10] The dynamics of relaxation of the first excited singlet state (S_1) of TPM dyes is seen to be very fast in low-viscosity solvents (on the order of few picoseconds) because of strong coupling between electronic states and torsional degrees of freedom. The nature of molecular electronic states of TPM dyes is strongly dependent on the angle between the central sp^2 carbon and the planes of phenyl rings. The relaxation time of the S_1 state of TPM dyes increases dramatically with increasing solvent viscosity (η), which follows an $\eta^{2/3}$ dependence and has been attributed to the radiationless decay due to the rotation of phenyl rings in solution.[11−15] A majority of the studies have concluded that there exists a nonfluorescent state S_x, or a vibrationally hot ground state, that is responsible for the ultrafast nonradiative deactivation of the S_1 state.[11−15] Among the vast number of TPM dyes, crystal violet (CV) and malachite green (MG) dyes have been considered to be the prototypes that represent the TPM dyes in their molecular symmetries; CV is close to a D_3 point group, and MG is close to a C_2 point group. In general, transient absorption, bleach recovery, and time-resolved fluorescence measurements have been used as the major tools in the study of the relaxation dynamics of the S_1 state of TPM dyes.[2,6,8,10]

The dynamics of the deactivation of higher excited states is of great importance in understanding the overall photophysics of a molecule, and a number of reviews concerning fast photophysical and photochemical processes in complex organic molecules have been reported.[16−19] However, there are still many unanswered fundamental questions concerning the mechanism and dynamics of radiationless transitions and vibronic relaxations including those from the higher excited electronic states. Recently, Mataga et al. have reported the dynamics of hot fluorescence emission from nonrelaxed vibronic states of Zn-tetraphenylporphyrin on excitation to the S_2 state.[17] In a recent communication, we demonstrated the role of nonequilibrated higher excited states in the relaxation dynamics of the tris-(2,2′-bipyridine) ruthenium(II) complex.[20] Contrary to general observation that fluorescence originates from the lowest excited state (Kasha's rule), MG displays fluorescence emission from the S_2 state, showing its significance in excited-state processes.[7,21] Efforts have been made in recent years to elucidate details of the relaxation dynamics of S_2 states in TPM dyes in comparison with its S_1-state dynamics. Yoshizawa et al. have observed a biexponential decay for the fluorescence from the S_2 state of MG in solution by fluorescence upconversion spectroscopy.[7] The faster component observed with a lifetime of ∼270 fs has been assigned to the equilibration of high-frequency internal modes, and the slower component (∼1.2 ps) is assigned to both the torsional configurational change and the internal conversion from the S_2 to the S_1 state.[7] Kanematsu et al. have recorded the time-resolved emission spectra of MG from

* To whom correspondence should be addressed. E-mail: cdscd@magnum.barc.ernet.in.
† Osaka University.
‡ Bhabha Atomic Research Centre.
§ Present address: Bhabha Atomic Research Centre. E-mail: bkac@apsara.barc.ernet.in.

10.1021/jp034486s CCC: $25.00 © 2003 American Chemical Society
Published on Web 04/04/2003

the S_2 state, which showed a dynamic Stokes shift in ethanol.[22] However, no further details have been provided. Apart from these studies, to the best our knowledge, no attempt has been made to explore the S_2-state dynamics in detail for MG and related dyes.

It is clear from the above discussion that the information on the mechanism and dynamics of radiationless transitions from higher excited states in TPM dyes is interesting from torsional dynamic aspects of the phenyl rings and for the applications of TPM dyes involving knowledge of the excited-state relaxation channels. In this work, we have employed femtosecond fluorescence upconversion method to explore the relaxation dynamics of the S_2 state of MG in solutions. The kinetic measurements at different wavelengths demonstrated cascade population relaxation within the S_2 potential surface with a time constant of ~130 fs, which is independent of solvent viscosity as seen in ethanol and ethylene glycol. Kinetic data along with time-resolved fluorescence anisotropy measurements at different emission wavelengths lead us to propose a relaxation pathway along an interaction of S_2 and S_1 potential surfaces forming a conical intersection, which leads to mixed vibrational levels of S_2 and S_1 characteristics. We propose that the conical intersection is along the torsional coordinate of the unsubstituted phenyl ring of the dye. Our proposal of a conical intersection between the S_2 and S_1 potential surfaces provides first-hand information on such a model in TPM dyes, which is substantially supported by time-resolved anisotropy measurements.

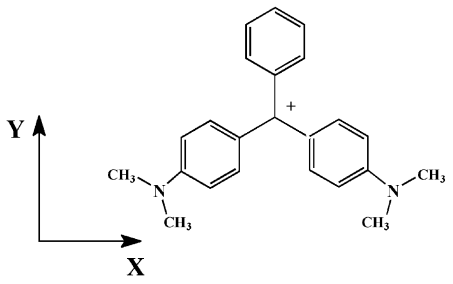

Malachite Green

2. Experimental Section

The cationic dye malachite green (oxalate) purchased from Exciton was used as received (structure shown). The solvents ethanol and ethylene glycol were purchased from Wako Chemicals, Japan (purity >99.5%) and were used as received. Steady-state absorption and fluorescence spectra were recorded on a Hitachi (U-3500) spectrophotometer and a Hitachi (850E) fluorimeter, respectively.

Fluorescence decays were measured by a femtosecond fluorescence upconversion setup described elsewhere.[20] Briefly, the setup is based on a Ti sapphire system (Tsunami, 70 fs, Spectra Physics) with an output of ~600 mW at ~820 nm with a repetition rate of 82 MHz. The second harmonic (SH) output was used to excite the sample held in a cell with a 1-mm path length. The polarization of the excitation beam was varied by introducing a half-wave plate into the pump beam line. For kinetic measurements, the excitation polarization was kept at the magic angle (54.7°), and for anisotropy measurements, it was rotated to 0 or 90° with respect to the gate pulse polarization. The sum frequency signals that were generated were collected and detected by an arrangement comprising lenses, a prism, spatial filters, a monochromator, and a photomultiplier tube in combination with a Stanford Research photon counter unit (SR400). The typical optical density of the sample at the excitation wavelength was ~0.5, which corresponds to a concentration of ~200 μM. During the measurements, flowing sample solutions were used to avoid any sample heating or decomposition. The excitation power applied to the sample was kept at ~10−12 mW. No excitation-power dependence was observed in the transient kinetics. The instrument response function was obtained from the cross correlation of the residual pump wavelength and the gate pulse, which gave the best fit to a Gaussian profile with a fwhm of ~130 fs.

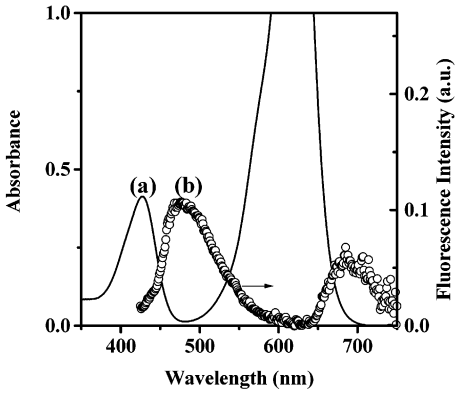

Figure 1. Ground-state absorption (a) and emission (b) spectra of malachite green in ethanol.

3. Results and Discussions

3.1. Steady-State Absorption and Fluorescence Measurements. The ground-state absorption spectrum of MG in ethanol (Figure 1) displays two visible absorption bands—one at ~620 nm with $\epsilon \approx 80\,000$ dm^3 mol^{-1} cm^{-1} and the other at 425 nm with $\epsilon \approx 17\,000$ dm^3 mol^{-1} cm^{-1}. These transitions are along the *x* and *y* axes of the molecular plane and are polarized orthogonal to each other (see structure).[1] The fluorescence emission spectrum recorded in ethanol solution on excitation at 410 nm is shown in Figure 1. Well-defined emission bands from the S_2 and S_1 states, which peak at 480 and ~680 nm, respectively, are observed. A similar spectrum has also been reported by Yoshizawa et al. by employing photon-counting detection.[7] Because of the strong ground-state absorption of MG in the 550−650-nm region, the emission spectrum in this region would not represent the actual profile. However, Figure 1 shows that the S_2 emission band is broad and has considerable overlap with the S_0-S_1 absorption band. This feature may hold implications for the relaxation dynamics in this molecule on excitation to higher excited levels. Attempts were made to obtain time-resolved information of the energy relaxation in MG by the fluorescence upconversion method, and the results have been presented in the following sections.

3.2. Time-Resolved Fluorescence Measurements. Relaxation processes in MG following the 410-nm excitation in ethanol solution were monitored by the fluorescence upconversion measurements. The decay traces recorded at different wavelengths within the S_2 and S_1 emission spectral region, 450−680 nm, are shown in Figure 2.

The trace at 450 nm (Figure 2a) displays a fast decay with a minor contribution from a slower component. Since the faster component decays with a rate comparable to the instrument time resolution, the decay constants were evaluated by convolution fitting where the decay trace $F(t)$ was fit by a convolution of the instrument response function $g(t)$ with a fitting function $f(t)$ that is an exponential function (eqs 1 and 2).[20]

$$F(t) = \int_{-\infty}^{t} g(t')\, f(t - t')\, \mathrm{d}t' \qquad (1)$$

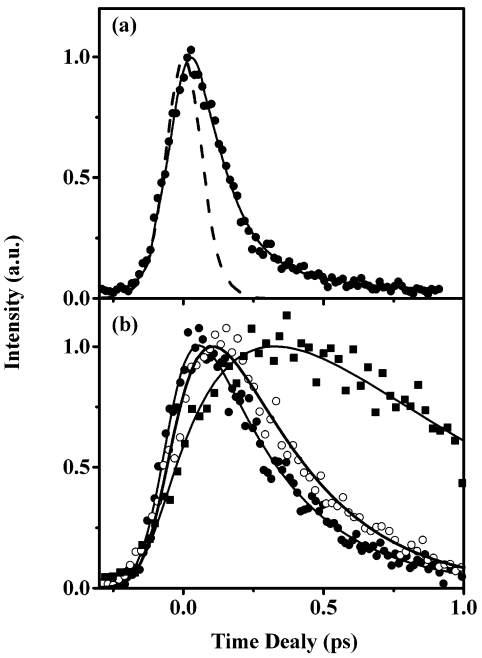

Figure 2. Fluorescence traces obtained in an ethanol solution of malachite green on excitation at 410 nm **(**a**)** at 450 nm (●).The solid line represent the best fit generated according to eqs 1 and 2, and the dashed line represents the instrument response function with a fwhm of 130 fs. **(b)** Traces obtained at 500 nm (●), 550 nm (○), and 680 nm (■). The solid lines represent the best fit generated according to eqs 1 and 3.

where

$$f(t) = A_1 \exp\left(-\frac{t}{\tau_1}\right) + A_2 \exp\left(-\frac{t}{\tau_2}\right) \qquad (2)$$

A_1 and A_2 represent the amplitudes, and τ_1 and τ_2 represent the lifetimes. The best convolution fit generated with lifetimes $\tau_1 = 130 \pm 15$ fs (96%) and $\tau_2 = 550 \pm 40$ fs (4%) is represented in the Figure as a solid line. Interestingly, the traces obtained at higher wavelengths displayed kinetic behavior that is different from that observed at 450 nm. Figure 2b shows the fluorescence signal monitored at 500 nm. It is seen that the trace could not be best fit with only the decay components; rather, it required a growth component as well. Assuming a cascade population relaxation of the emitting states, the fitting analyses were carried out on the basis of the following functional form, $f(t)'$, in eq 1:

$$f(t)' = A_1\left[\exp\left(-\frac{t}{\tau_d}\right) - \exp\left(-\frac{t}{\tau_r}\right)\right] \qquad (3)$$

τ_r and τ_d represent the growth and decay times, respectively. Following eqs 1 and 3, the analysis of the trace recorded at 500 nm provided 60 ± 10 fs as the growth time and 297 ± 20 fs as the decay time. Interestingly, the kinetic profile obtained at other wavelengths within the S_2 band displayed a slower growth time. At 550 nm (Figure 2b), the kinetic analysis rendered 130 ± 15 and 265 ± 20 fs as the rise and decay times, respectively. Similar time constants have been obtained at 600 nm, though the signal-to-noise ratio was poor at this wavelength. However, at wavelengths above 650 nm, which mainly represents the S_1 emission band, the growth and decay processes provided lifetimes of 290 ± 25 and 800 ± 60 fs, respectively. The fluorescence trace recorded at 680 nm, along with the fit generated according to eqs 1 and 3, is displayed in Figure 2b (solid line).

Yoshizawa et al. have investigated the relaxation of the S_2 excited state of MG by using fluorescence upconversion spectroscopy with an instrument resolution of 280 fs.[7] The decay kinetics of the S_2 state that they monitored at 490 nm displayed single-exponential decay in solvents of low viscosity whereas the decays were biexponential in more viscous solvents such as ethylene glycol. The faster decay (~230 fs) has been assigned to the equilibration of high-frequency internal modes in the S_2 state, some of which relax directly to the S_1 state. However, no observation has been made on the wavelength-dependent kinetic changes within the S_2 band. Our experiments with better time resolution (~130 fs fwhm) provide a kinetic profile at 450 nm having a faster decay (~130 fs) compared to that observed at 490 nm by Yoshizawa et al.[7] Thus, it would be more appropriate to assign this faster decay component to the relaxation of the high-frequency internal modes in S_2, contrary to the assignment of Yoshizawa et al. However, this assignment does not explain the differences in the growth and decay kinetics that are observed in Figure 2. Vibrational relaxation can appear as fast decay components in fluorescence decay traces, but the observation of a corresponding growth component in such processes is quite unusual.[10,17] However, it is probable that owing to the strong absorption of the ground state of the dye in the 550-nm region the monitored photons can appear at a delayed time because of emission occurring from reabsorption, in turn presenting a slower growth time. This possibility has been checked by using different concentrations of the dye and has been verified so that no such experimental artifact contributes to the signal observed here.

The present results on the kinetics within the S_2 emission band clearly show that the S_2-state dynamics in MG involves more interesting and complex deactivation phenomena than those discussed in the literature.[7,22] The intricacy of the S_2-state relaxation was analyzed in line with that of the S_1-state relaxation. As discussed earlier, TPM dyes are known to undergo ultrafast nonradiative decay from the S_1 state, which involves the rotational motion of the phenyl rings on a barrierless potential surface.[11−15] Such relaxations are seen to be dependent on solvent viscosity and have been discussed on the basis of several models.[23] The effect of viscosity on the relaxation processes has been examined by employing ethylene glycol ($\eta = 26.09$) instead of ethanol ($\eta = 1.08$) as the solvent. The decay traces followed at 450 nm in ethylene glycol did not show any variation in the faster decay time, but an increase in the contribution of the slower component has been observed. The faster component displayed a lifetime of ~130 fs whereas the slower component has an ~825 fs decay time with a 25% contribution. However, no appreciable changes were observed in the growth kinetics at 500, 550 nm, and so forth on changing the solvent from ethanol to ethylene glycol. In the case of the S_2 state, on the basis of the fluorescence decay kinetics observed at 490 nm, Yoshizawa et al. claimed that the slower component observed in the biexponential fitting corresponds to a change in the torsional configuration in low-viscosity solvents, which shifts to an internal conversion process on increasing the solvent viscosity.[7] Recently, Kanematsu et al. reported a dynamic Stokes shift in the S_2-S_0 fluorescence of MG in ethanol by employing Kerr-gate fluorescence spectroscopy.[22] However, no further details have been provided on the solvent polarity/viscosity effects.

The above-mentioned features of the fluorescence decay strongly indicate that the relaxation of the S_2-state kinetics observed within the emission band represents a relaxation process that is almost independent of the solvent viscosity as

observed in ethanol and ethylene glycol. As an alternative approach to this problem, experiments have been conducted with a polarized excitation pulse. In the case of bulky TPM dyes, the rotational depolarization time in water is ~200 ps, which is much slower than the dynamics observed here.[24] Hence, the measurement of fluorescence anisotropy would be a suitable choice to provide more insight into the relaxation dynamics observed here.

3.3. Fluorescence Anisotropy Measurements. Fluorescence anisotropy is determined by the angle between the transition moments for the absorption and emission, which reveal the average angular displacement of the fluorophore that occurs between absorption and subsequent emission of photons and is given by

$$r = \frac{2}{5}\left(\frac{3\cos^2\beta - 1}{2}\right) \quad (4)$$

where β is the angle between the excitation and emission transition dipoles.[25,26] For collinear absorption and emission transitions, the value of r is 0.4. Reductions from 0.4 reflect changes in the emission transition dipole and can be well correlated to the structural orientations. In general, fluorescence anisotropy is independent of emission wavelength because the emission occurs from the relaxed excited states. Since the S_2 and S_1 transition moments in MG are orthogonal to each other, one would expect anisotropy values close to 0.4 or −0.2 (eq 4) for the S_2 and S_1 states, respectively. However, if emission occurs from other excited states or in the presence of mixed levels of different excited states, the emission anisotropy may represent wavelength-dependent behavior.

As mentioned in the Experimental Section, the fluorescence traces were obtained on maintaining the excitation polarization parallel or perpendicular to the gate pulse. From these traces, the time-dependent anisotropy, $r(t)$, values have been evaluated from eq 5.[25]

$$r(t) = \frac{I_{II}(t) - I_{\perp}(t)}{I_{II}(t) + 2I_{\perp}(t)} \quad (5)$$

where $I_{II}(t)$ and $I_{\perp}(t)$ refer to the intensities of the fluorescence profile obtained with excitation polarization parallel and perpendicular to the gate pulse, respectively. The time-dependent anisotropy values thus calculated at different wavelengths along the S_2 and S_1 emission bands on excitation at 410 nm are presented in Figure 3.

At 450 nm (Figure 3a), the anisotropy starts from 0.38 and decays quickly to a steady value of ~0.3. However, the $r(t)$ value at 500 nm (Figure 3b) is 0.275, which did not show any significant change in the time window that was monitored. At 550 nm (Figure 3c), the anisotropy is reduced to 0.225, and at 600 nm, this is only 0.2. Notable changes have been observed for wavelengths longer than 650 nm. The $r(t)$ values obtained at 680 nm (Figure 3d) and the wavelength that represents the S_1 band clearly manifest anisotropy decay from 0 to −0.1. In a qualitative estimation, this anisotropy decay is found to be single-exponential with a time constant of ~300 fs. A similar anisotropy pattern has been observed at 740 nm.

It is known that the time-dependent anisotropy values calculated with signals convoluted with the instrument response do not represent the actual values, particularly when the time-dependent changes are close to the time resolution of the instrument.[27] In the present case, anisotropy values at different wavelengths were also calculated by using a deconvoluted fitted

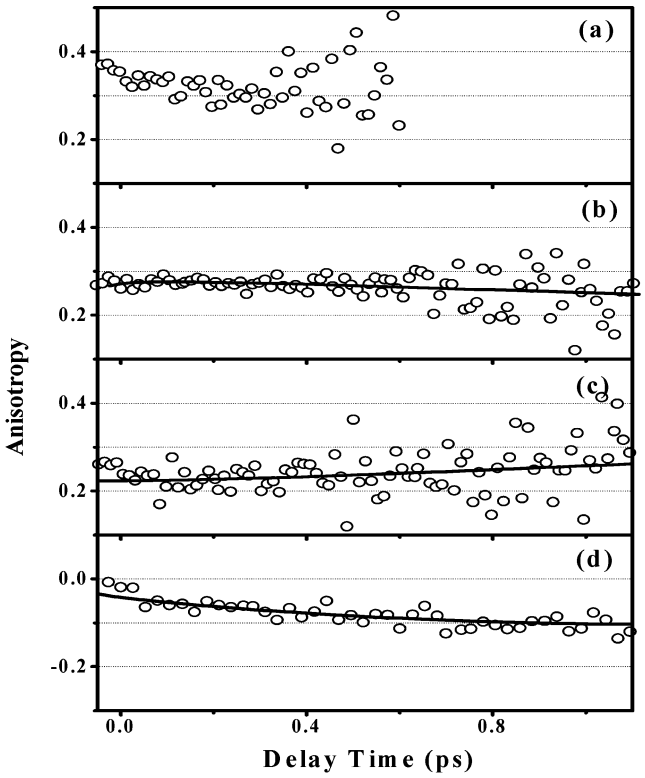

Figure 3. Time-dependent anisotropy values (○) recorded at 450 nm (a), 500 nm (b), 550 nm (c), and 680 nm (d) on excitation at 410 nm in an ethanol solution of malachite green. The solid lines represent the anisotropy calculated after deconvoluting the instrument response function.

trace. It was seen in all of the cases except the one at 450 nm that the time-dependent anisotropy calculated without deconvoluting the instrument response agrees well with the value obtained after deconvoluting the response function. The anisotropy values calculated after deconvoluting the instrument response function are shown in Figure 3 as solid lines. It should be noted here that the kinetics at 450 nm is faster than that at other wavelengths, so the $r(t)$ calculated after deconvoluting the instrument response function did not match the values presented in Figure 3a.

Yoshizawa et al. have reported anisotropy values of 0.26 and −0.08 for the S_2 and S_1 states, respectively, by exciting MG in ethanol at 400 nm.[7] However, no time dependence or wavelength dependence has been probed. Though values reported by them match our results obtained at 500 and 680 nm on a longer time scale, the interesting dynamic aspects of the anisotropy decay are missing in their experiments. Wavelength-dependent anisotropy changes on photoexcitation of aluminum-(III) tris(8-hydroxyquinoline) (Alq_3) have been reported.[28] These changes have been discussed on the basis of a solvation process where on photoexcitation of Alq_3 a solvation-induced mixing of nearby excited electronic states of different radiative character takes place.[28] Different directions for the optical dipole transition moments of the admixed states will then lead to temporal changes in anisotropy as the solvation progresses. However, in the present study, the results obtained in solvents of different polarity and viscosity did not indicate any such evidence attributable to the solvation process in the S_2 state.

In the present case, the anisotropy value is also seen to decrease gradually on monitoring at longer wavelengths. Also, temporal evolution has been observed at 450 nm and at wavelengths above 650 nm (Figure 3). In line with the work of

Veldhoven et al. on Alq_3, the anisotropy change observed here within the S_2 band could arise from a spectral overlap within the S_2 absorption band, where the emissive state is populated by relaxation from different electronic excited states.[28] Consequently, the directional correlation between the absorption and emission dipoles is partially lost, and values for $r(0)$ lower than 0.4 will be obtained. However, experimentally it has been seen that the emission spectrum did not show any dependence on the excitation wavelength within the S_2 band. However, a reduction in the anisotropy can also result from a mixing of nearby excited electronic states of different radiative character. This could arise from two possibilities. First, one considers two diabatic states with weakly avoided touching of the Landau−Zener type, and the second one is a relaxation through a unique point on a multidimensional reaction surface, leading to surface touching of the S_2 and S_1 states (i.e., a conical intersection (CI)).[29−35] Since the measured lifetime for S_2 fluorescence is very fast (<300 fs), it is more probable that the relaxation occurs through a conical intersection. The presence of a CI results in admixed levels of both S_2 and S_1 states, as revealed in the anisotropy measurements. However, the contribution from the former possibility cannot be totally ignored.

Conical intersections have been implicated in the mechanisms of many ultrafast excited decay processes.[29−35] Many photochemical reactions follow pathways necessitating large-amplitude coordinates that are typically connected with conical intersections. In such models, the excited-state decay is not through the energy levels of rigid conformers; rather, it follows a pathway along various intramolecular motions, allowing a continuous transition between the energy levels. In a recent report on the excited-state dynamics of a julolidino analogue of crystal violet, another TPM dye, relaxation via a conical intersection between the S_1 and S_0 potential surfaces involving the torsional motion of two of the phenyl rings has been proposed.[36]

It may be noted here that in the case of MG the charge migration accompanying the S_2 transition is essentially confined to the migration of electrons from the phenyl ring bearing no substituents to the rest of the system whereas the S_1 band transition is localized on the central carbon atom and the two phenyl rings bearing the substituent groups (see structure).[1] Thus, it is reasonable to assume that on excitation to the S_2 state the unsubstituted phenyl ring brings about a favorable reaction coordinate, which leads to the conical intersection of the S_2 and S_1 states. Along with the change in the torsional angle of the unsubstituted phenyl ring (one of the coordinates), the angle between the two phenyl rings carrying the substituents may also change, providing the second coordinate to establish a conical intersection.

Following the above discussion, the relaxation mechanism in MG following the S_2-state excitation can be summarized as shown in Figure 4. Excitation at 410 nm takes the molecule to higher levels in the S_2 state. Immediate relaxation can be monitored at 450 nm and has been found to be fast (∼130 fs). Correspondingly, the growth of the lower levels in the S_2 state has been seen at 500 and at 550 nm, which showed good agreement with the decay of the initially excited state. As represented in Figure 4, the excited molecule moves along the potential energy surface provided by the torsional coordinate of the phenyl ring and is dragged quickly toward the conical intersection, ending up in admixed levels of both S_2 and S_1 states (shown as the shaded portion in the scheme). Experimentally, this process is seen as a successive reduction in anisotropy toward longer wavelengths within the S_2 emission profile.

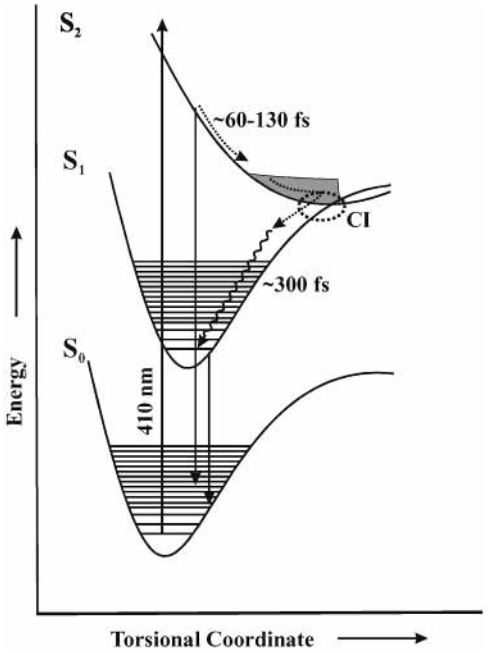

Figure 4. Schematic representation of the proposed relaxation pathways in malachite green. CI represents the conical intersection.

At the conical intersection point, the population represents an equal distribution of both parallel and perpendicularly polarized molecules, and the anisotropy is expected to be zero. This is manifested in the anisotropy traces obtained for the S_1 band where the $r(t)$ value starts from zero—the CI point. Through the CI, the molecule crosses over to the S_1 surface, which undergoes internal conversion to its lower levels. This corresponds to the formation time observed for the S_1 state. In general, one would expect an anisotropy of −0.2 for the S_1-state emission upon S_2-state excitation. However, the presence of CI and a slower rate of internal conversion in the S_1 state (∼300 fs) could be the reason for the observation of an anisotropy decay at 680 nm (S_1 band). The growth kinetics of S_1 state and the anisotropy decay provided more or less similar time constants, indicating that either internal conversion or orientational change could be the rate-determining step for the growth of the S_1 population. It has been observed that the 450-nm decay showed a slower component with an increased contribution in viscous solvents. This could be assigned to a fraction that populates the S_1 state without following the CI point.

Though the dynamics of relaxation of S_1 states in TPM dyes has been well studied, it is presumed that the results presented here give direct information on the interesting excited-state dynamics of a typical TPM dye (i.e., MG in its S_2 state). Our ongoing experiments dealing the excitation-energy dependence in some of the TPM dyes (e.g., malachite green and brilliant green in different alcohol solvents) will surely provide a clearer picture of this interesting relaxation dynamics. Correlation of the structural aspect with the relaxation dynamics will be discussed. Considering the complexity of the molecular system, it is difficult to provide any theoretical support for the results presented here at this stage; however, efforts are underway from our side to obtain information on the structural aspects and potential energy surfaces of the levels involved using an ab initio method.

In conclusion, the relaxation dynamics of the S_2 state of a TPM dye, malachite green, has been studied by femtosecond fluorescence upconversion spectroscopy. The initial relaxation

is seen to be faster than that recently reported by Yoshizawa et al. The kinetic measurements at different wavelengths suggested a cascade population relaxation along the S_2 state with a time constant of ~130 fs that is almost independent of solvent viscosity, contrary to the relaxation dynamics of the S_1 state. Wavelength-dependent time-resolved anisotropy measurements along the S_2 and S_1 emission bands displayed successive reductions in the anisotropy values, indicating a continuous evolution of the S_1 surface without any energy gap. Detailed analysis leads us to propose a relaxation pathway along an interaction of S_2 and S_1 potential surfaces (i.e., the conical intersection), which leads to mixed vibrational levels of S_2 and S_1 characteristics. It is proposed that the conical intersection is promoted by the torsional coordinate of the unsubstituted phenyl ring of the dye, where the S_2 transition energy is localized. Our proposal of a conical intersection between the S_2 and S_1 potential surfaces provides first-hand information on such a model in TPM dyes, which is substantially supported by time-resolved anisotropy measurements.

References and Notes

(1) Duxbury, D. F. *Chem. Rev.* **1993**, *93*, 381.

(2) Ishikawa, M.; Ye, J. Y.; Maruyama, Y.; Nakatsuka, H. *J. Phys. Chem. A* **1999**, *103*, 4319.

(3) Bhasikuttan, A. C.; Sapre, A. V.; Rama Rao, K. V. S.; Mittal, J. P. *Photochem. Photobiol.* **1995**, *62*, 245.

(4) Bhasikuttan, A. C.; Shastri, L. V.; Sapre, A. V. *J. Photochem. Photobiol., A* **1998**, *112*, 179.

(5) Nagasawa, Y.; Ando, Y.; Okada, T. *Chem. Phys. Lett*. **1999**, *312*, 161.

(6) Nagasawa, Y.; Ando, Y.; Kataoka, D.; Matsuda, H.; Miyasaka, H.; Okada, T. *J. Phys. Chem.* A **2002**, *106*, 2024.

(7) Yoshizawa, M.; Suzuki, K.; Kubo, A.; Saikan, S. *Chem. Phys. Lett*. **1998**, *290*, 43.

(8) Martin, M. M.; Plaza, P.; Meyer, Y. H. *J. Phys. Chem*. **1991**, *95*, 9310.

(9) Cremers, D. A.; Windsor, M. W. *Chem. Phys. Lett*. **1980**, *71*, 27.

(10) Mokhtari, A.; Chebira, A.; Chesnoy, J. *J. Opt. Soc. Am*. **1990**, *B7*, 1551.

(11) Sundstrom, V.; Gillbro, T.; Bergstrom, H. *Chem. Phys*. **1982**, *73*, 439.

(12) Sundstrom, V.; Gillbro, T. *J. Chem. Phys*. **1984**, *81*, 3463.

(13) Ben-Amotz, D.; Harris, C. B. *J. Chem. Phys.* **1987**, *86*, 4856.

(14) Ben-Amotz, D.; Harris, C. B. *J. Chem. Phys.* **1987**, *86*, 5433.

(15) Ben-Amotz, D.; Jeanloz, R.; Harris, C. B. *J. Chem. Phys*. **1987**, *86*, 6119.

(16) Ermolaev, V. L. *Russ. Chem. Rev. (Engl. Transl.)* **2001**, *70*, 471.

(17) Mataga, N.; Shibata, Y.; Chosrowjan, H.; Yoshida, N.; Osuka, A. *J. Phys. Chem. B* **2000**, *104*, 4001.

(18) Fujino, T.; Arzhantsev, S. Y.; Tahara, T. *Bull. Chem. Soc. Jpn.* **2002**, *75*, 1031.

(19) Elsaesser, T.; Kaiser, W. *Annu. Rev. Phys. Chem*. **1991**, *42*, 83.

(20) Bhasikuttan, A. C.; Suzuki, M.; Nakashima, S.; Okada, T. *J. Am. Chem. Soc*. **2002**, *124*, 8398.

(21) Janowski, A.; Rzeszotarska, J. *J. Lumin.* **1980**, *21*, 409.

(22) Kanematsu, Y.; Ozawa, H.; Tanaka, I.; Kinoshita, S. *J. Lumin*. **2000**, *87*−*89*, 917.

(23) Bagchi, B.; Fleming, G. R.; Oxtoby, D. W. *J. Chem. Phys*. **1983**, *78*, 7375.

(24) Lueck, H. B.; McHale, J. L.; Edward, W. D. *J. Am. Chem. Soc.* **1992**, *114*, 2342.

(25) Lakowicz, J. R. *Principles of Fluorescence Spectroscopy*, 2nd ed.; Kluwer Academic/Plenum Publishing: New York, 1999; Chapters 10 and 11.

(26) Saikan, S.; Sei, J. *J. Chem. Phys.* **1983**, *79*, 4146.

(27) Papenhuijzen, J.; Visser, A. J. W. G. *Biophys. Chem*. **1983**, *17*, 57.

(28) Veldhoven, E. V.; Zhang, H.; Glasbeek, M. *J. Phys. Chem. A* **2001**, *105*, 1687.

(29) Michl, J.; Bonacic-Koutecky, V. *Electronic Aspects of Organic Photochemistry*; Wiley-Interscience Publications: New York, 1990; Chapter 2.

(30) Bernardi, F., Olivucci, M., Robb, M. A. *Chem. Soc. Rev*. **1996**, *25*, 321.

(31) (a) Michl, J. *Top. Curr. Chem*. **1974**, *46*, 1. (b) Michl, J. *J. Mol. Photochem*. **1972**, 243, 257.

(32) Seidner, L.; Stock, G.; Sobolewski, A. L.; Domcke, W. *J. Chem. Phys*. **1992**, *96*, 5298.

(33) Woywod, C.; Domcke, W.; Sobolewski, A. L.; Werner, H. J. *J. Chem. Phys.* **1994**, *100*, 1400.

(34) Heider, N.; Fischer, S. F. *Chem. Phys*. **1984**, *88*, 209.

(35) Fuss, W.; Lochbrunner, S.; Muller, A. M.; Schikarski, T.;. Schmid, W. E.; Trushin, S. A. *Chem. Phys*. **1998**, *232*, 161.

(36) Jurczok, M.; Plaza, P.; Martin, M. M.; Rettig, W. *J. Phys. Chem. A* **1999**, *103*, 3372.